Scaling Interface Length Increase Rates in Richtmyer–Meshkov Instabilities

V. Kilchyk
Department of Mechanical Engineering,
Indiana University–Purdue University,
723 West Michigan Street,
Indianapolis, IN 46202;
Department of Mechanical Engineering,
Purdue University,
585 Purdue Mall,
West Lafayette, IN 47907

R. Nalim
Department of Mechanical Engineering,
Indiana University–Purdue University,
723 West Michigan Street,
Indianapolis, IN 46202

C. Merkle
Department of Mechanical Engineering,
Purdue University,
585 Purdue Mall,
West Lafayette, IN 47907

The interface area increase produced by large-amplitude wave refraction through an interface that separates fluids with different densities can have important physiochemical consequences, such as a fuel consumption rate increase in the case of a shock–flame interaction. Using the results of numerical simulations along with a scaling analysis, a unified scaling law of the interface length increase was developed applicable to shock and expansion wave refractions and both types of interface orientation with the respect to the incoming wave. To avoid a common difficulty in interface length quantification in the numerical tests, a sinusoidally perturbed interface was generated using gases with different temperatures. It was found that the rate of interface increase correlates almost linearly with the circulation deposited at the interface. When combined with earlier developed models of circulation deposition in Richtmyer–Meshkov instability, the obtained scaling law predicts dependence of interface dynamics on the basic problem parameters. [DOI: 10.1115/1.4023191]

Keywords: shock refractions, rarefaction wave refraction, expansion wave refraction, Richtmyer–Meshkov instability, density interface, baroclinic vorticity, shock–flame interaction, flame stretch, flame-vortex interaction, mixing

1 Introduction

The oblique propagation of a pressure wave through a density discontinuity or gradient region results in baroclinic vorticity production that is evidenced by a vortex sheet. These vortex sheets, in turn, induce local fluid motion at the interface between fluids of different densities, leading to the deformation of this interface through a process known as Richtmyer–Meshkov (R–M) instability. The time evolution of the interface in this process has been studied analytically using zero-dimensional analyses, an example of which includes the perturbation amplitude growth (Fig. 1) on the interface between impulsively accelerated fluids of different densities [1–5]. For various practical problems such as the prediction of the flame chemical reaction rate, species transport, or gas mixing in multiple physical problems involving the R–M instability, the interface length change is ultimately more important than the perturbation amplitude growth [6–10]. However, the interface increase takes place in two or three dimensions with interface roll-ups produced by a vortex-like flow field (Fig. 1). This creates significantly different growth patterns of interface length and perturbation amplitude (Fig. 2). One example of such a problem is shock–flame interaction where density discontinuity also coincides with a chemical reaction front. In this problem, the flame length is the most crucial parameter defining the fuel consumption rate. Moreover, most of the existing R–M instability analysis is restricted to the shock refractions, while it is well known that expansion waves also produce an interface deformation similar to that of shocks [11]. Therefore, in this work we investigate the rates of interface increase following shock or expansion wave refractions in both types of refractions (fast/slow and slow/fast).

This paper is organized as follows. First, the computational setup and code validation is described in Sec. 2, followed by a brief summary of the numerical tests in Sec. 3. Then, using the numerical results, a unified scaling law is proposed in Sec. 4.

Manuscript received February 25, 2012; final manuscript received December 7, 2012; published online February 22, 2013. Assoc. Editor: Ye Zhou.

2 Numerical Approach

Computational Setup. Numerical solutions to the two-dimensional (2D) nonreactive Navier–Stokes equations along with the continuity, energy, and species equations were obtained using an in-house CFD code (GEMS) that was extensively validated by comparison with experimental and analytical results [12–15]. Second-order finite-volume spatial discretization and three-point backward differencing were used for the temporal discretization. Spatial discretization was achieved by a generalized Riemann approach for the convective terms along with a Galerkin approach for the diffusive terms. A Barth limiter [16] was employed in the face fluxes. An implicit multilevel pseudo-time marching method was used to eliminate factorization errors. A sample convergence at each time step in unsteady calculations is presented in Fig. 3.

A schematic of the problem setup is shown in Fig. 4. The shock or expansion wave is propagated along a channel through a sinusoidally perturbed density interface. The symmetry of the general problem (Fig. 1) allowed modeling of only half of the sine wave. The grid was refined in the central part of the computational domain. Initial parameters are provided in Table 1. Domain length (up to $\sim$7 m) was selected to avoid repeated interaction with reflected from the inlet or outlet shock/expansion waves. To ensure that the interface remained within the refined part of the domain after the refraction, an initial velocity was applied (Fig. 4). Symmetry boundary conditions were applied on the left and right sides of the computational domain. Flow-through boundary conditions (changing from the inlet to outlet according to the direction of the velocity in the interior cells) were applied at the two ends of the channel.

There is a possible difficulty associated with the length measurements of the multiscale interface deformation. After the shock/expansion wave refraction, smaller and smaller scale features evolve over time. The minimum size of these features is limited only by the combined physical and numerical viscosity. To avoid the difficulty of the interface length definition of a fractal-like multiscale structure, the problem may be redefined in conformity with its key practical counterpart—shock-flame interaction. The interface, in such a case, is generated by gases with different temperatures. The action of heat diffusion prevents the development

 Copyright © 2013 by ASME

Downloaded From: http://fluidsengineering.asmedigitalcollection.asme.org/ on 02/25/2014 Terms of Use: http://asme.org/terms

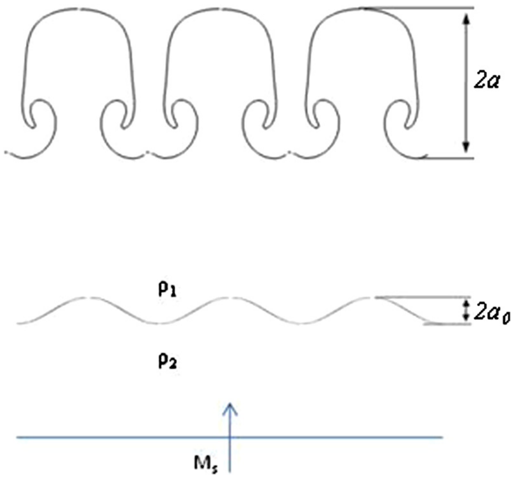

Fig. 1 A schematic of the sinusoidal interface evolution following shock refraction. Initial interface was produced as $y = a_o \sin(2\pi x/\lambda)$.

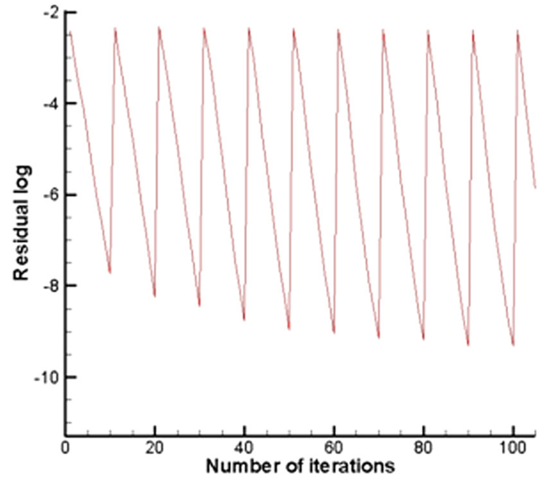

Fig. 3 Normalized residual unsteady calculations in a fast/slow M1.5 shock refraction. Every physical time step has 10 inner iterations.

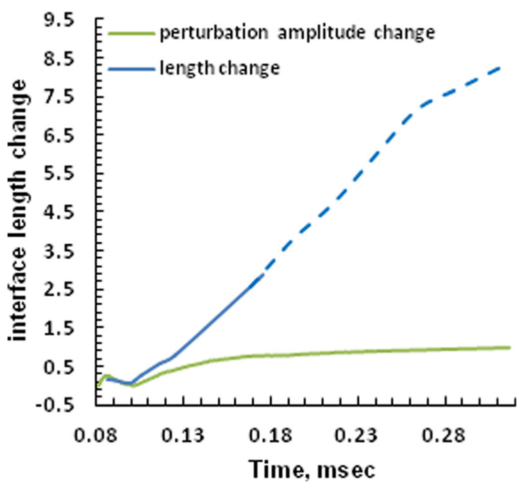

Fig. 2 Typical interface length and perturbation amplitude change in a Richtmyer–Meshkov instability (fast/slow Mach 1.7 shock, all values are normalized by the initial interface length)

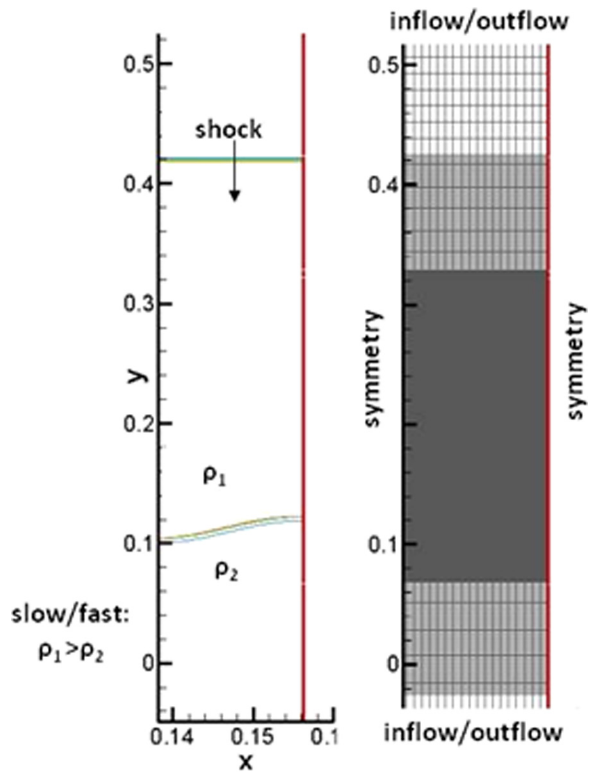

Fig. 4 The numerical setup (*a*) and grid (*b*) for the two-dimensional computations. Dimensions are scaled by a reference length of 0.5 m.

of perturbations below a certain scale, called inner cutoff. It is comparable to the laminar flame thickness, which is ∼0.5 mm for most cases [17,18]. The main motivation of this work is the analysis of the flame-pressure wave interaction [8,9,19–21]; therefore the temperature and the density ratios across the interface (2380 K/300 K and $\rho_{\text{fast}}/\rho_{\text{slow}} = 0.129$) and the gas composition were chosen to correspond to a stoichiometric propane flame under standard conditions.

We adopted the terminology of fast/slow and slow/fast refractions similar to that in previous works [22,23]. This terminology is related to the interface orientation in terms of the acoustic impedances (ρc) on each side with respect to the incoming wave. The relative magnitude of the impedances across the interface is one of the key parameters in determining the type of the refraction. In problems like combustion, with a limited range of density ratios, the relative magnitude of the speed of sound across the interface defines the acoustic impedance ratio. Thus, the terms "fast" or "slow" may simply refer to the interface side with the faster or slower speed of sound.

Gas properties with variable specific heats were used in the computations. Some of the problem parameters are shown in Table 1.

Table 1 Gas properties

Definition	Value
Initial Atwood number (A)	0.77
Grid size, mm	0.15
Specific heat ratio of the gas	1.36
Amplitude-to-wave length ratios (a_o/λ)	0.5, 0.375, 0.25, 0.125
Wave length (λ), cm	1.85

Length Computation. To compute the density interface length, a post-processing algorithm was developed and tested

Downloaded From: http://fluidsengineering.asmedigitalcollection.asme.org/ on 02/25/2014 Terms of Use: http://asme.org/terms

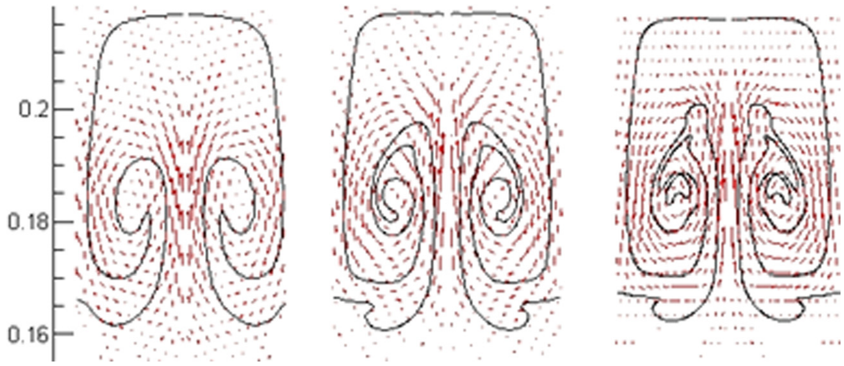

Fig. 5 Density interface in a Mach 1.5 shock density interaction at 0.33 msec in the computation with three grid resolutions: (*a*) 24,090, (*b*) 64,561, and (*c*) 222,580 nodes ($a_o/\lambda = 0.5$). Dimensions are scaled by a reference length of 0.5 m.

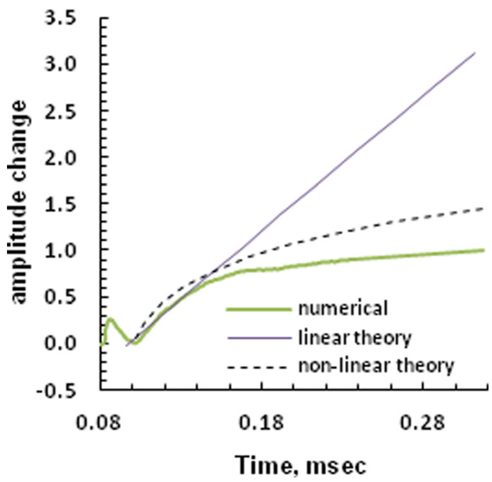

Fig. 6 Comparison of analytically predicted and numerical results for the perturbation amplitude change in a fast/slow Mach 1.7 shock refraction over a sinusoidal interface ($a_o/\lambda = 0.25$). Values are normalized by the initial interface length (interface length of a half wave 1.38 cm).

against the known geometries. The interface was represented by the iso-concentration line of C_3H_8 mass fraction = 0.03. In the algorithm, the interface length was computed by summing the small segment-connecting points along this iso-concentration line. This technique may fail when the interface breaks into parts or develops closed segments. Thus, after such a moment was reached, the interface length was computed manually from printed concentration maps using a map measurer. To verify algorithm accuracy, the computed length was compared with the exact values for the different curves. The error was estimated to be under ±2% of the actual length, while the error of the manual measurement using the curvimeter was estimated to be within ±2.5%.

To establish grid independence, three grid resolutions with $\Delta x = \Delta y = 0.3$, 0.15, and 0.075 mm in the refined part were tested. The density interface after a prescribed time is shown in Fig. 5, indicating that the finer grid created a somewhat slower perturbation growth. Additionally, gas motion in the finer grid cases produced a less-viscous motion, promoting rotation in the center of the domain that increased the interface length. The grid refinement was done in two steps, increasing the resolution from 0.3 to 0.15 and from 0.15 to 0.075 mm, and changed the values of the deposited circulation by 1.97% and 0.5%, respectively, while the interface length changed by 14.5% and 4.5%. Considering that the last change approaches the accuracy of the length measurements, a resolution of a 0.15 mm cell grid was deemed satisfactory for the computations and comparable to the ones used by others [9,19,23]. The selected grid resolution was equal to or better than the ones used in other reported shock-flame interaction studies [19].

To validate the code, flow properties and vortex sheet strength after shock and expansion wave refractions were compared with analytically calculated values [15,24]. The difference between the numerical and the analytical results was within 2% of the analytical solution. Furthermore, numerically computed values of perturbation amplitude growth were compared with the analytically predicted values using Richtmyer's expression [5] and the

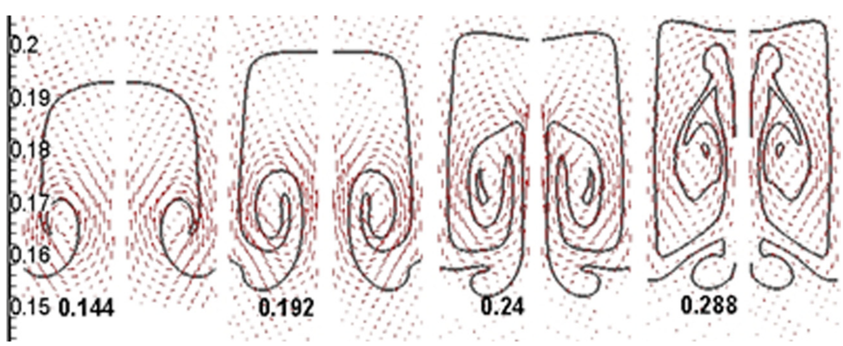

Fig. 7 Interface evolution following Mach 1.7 shock fast/slow refraction ($a_o/\lambda = 0.25$). Time is shown in milliseconds at the bottom. Dimensions are shown in $0.5 \times$ m.

Downloaded From: http://fluidsengineering.asmedigitalcollection.asme.org/ on 02/25/2014 Terms of Use: http://asme.org/terms

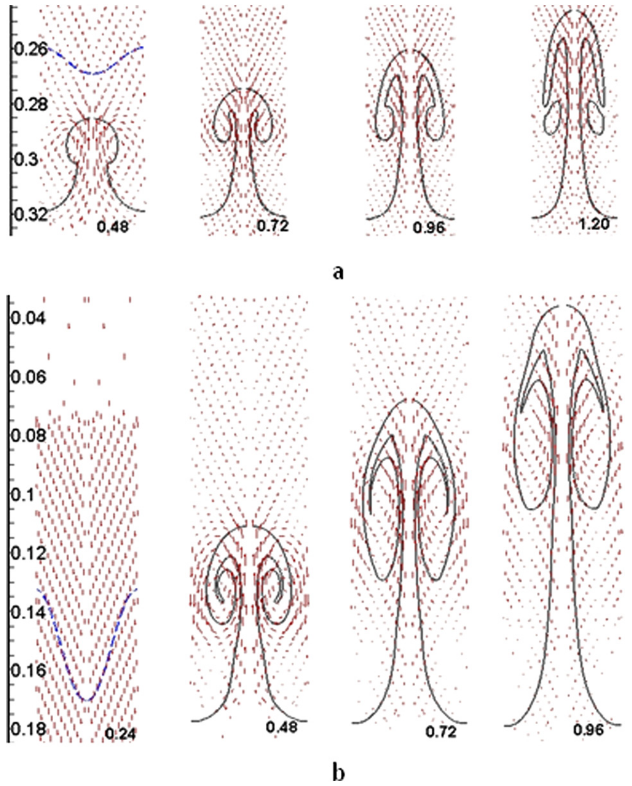

Fig. 8 Interface evolution following Mach 1.5 shock slow/fast refraction at interface with *a* - 0.125 and *b* - 0.5 amplitude-to-wavelength ratio (a_o/λ). Initial interface profile is shown with a dashed line. Time is shown in milliseconds at the bottom. Dimensions are shown in 0.5 × m.

nonlinear theory developed by Sadot [25] (Fig. 6). All the values were normalized by the initial length of the interface. As can be seen in Fig. 6, the numerically and analytically computed results demonstrated a reasonable correlation of 5–10% until 0.17 msec, when motion became very slow due to viscous effects.

3 Numerical Results

A typical computed interface dynamic is shown in Fig. 7. Initially sinusoidal, it develops into a mushroom-like shape common to R–M instability (Figs. 7 and 8). Plotted velocity vectors show that the interface becomes engaged in the vortex-like flow field. Rotation and translation of these vortices stretches and later breaks (~0.28 msec) the interface. The corresponding interface length change (the difference in interface length normalized by its initial value) is plotted in Fig. 9. The plotted results include the interface increase produced by the refractions of Mach 1.1–1.7 shocks and expansion waves with 1.05–1.245 pressure ratios ($a_o/\lambda = 0.25$). A small contraction of the interface may be noticed at the beginning. This contraction is due to the gas compression creating a short-term negative interface increase rate and the interface reversing in the slow/fast cases. Most importantly, the interface length changes at a nearly constant rate for a time period exceeding the linear perturbation amplitude growth. A similar behavior was observed in the expansion wave refractions, shown in Fig. 10. The plotted results also show that weak shocks and expansion waves produced comparable interface increase rates for waves with the same pressure ratios (Fig. 10). The larger, faster interface length increase was generated by the shocks in fast/slow refractions and by the expansion waves in slow/fast refractions. The summary of the results is shown in Table 2. All the results in the table correspond to half-wavelength.

The refraction generated circulation may be considered to be one of the problem parameters and is provided along with the interface velocity growth rate (of the half-wavelength) in Table 2. In addition, the table includes the interface velocity jump (Δv) that was calculated using an iterative solution similar to the one described earlier in Ref. [15].

One of the difficulties is in quantifying the shock/expansion wave deposited circulation that is responsible for the observed interface growth. Due to the so-called secondary vorticity deposition [26], circulation keeps rapidly increasing for a considerable amount of time after an incident wave passes an interface. The term *secondary* mainly implies that circulation is generated during the repeated interactions with secondary waves.

Since the studied problem is related to the infinite interface (due to the symmetrical boundary conditions on both sides of the domain), such waves originated from the other refractions. The term secondary vorticity is somewhat artificial since the secondary interactions may also be linked to the initial refraction and would

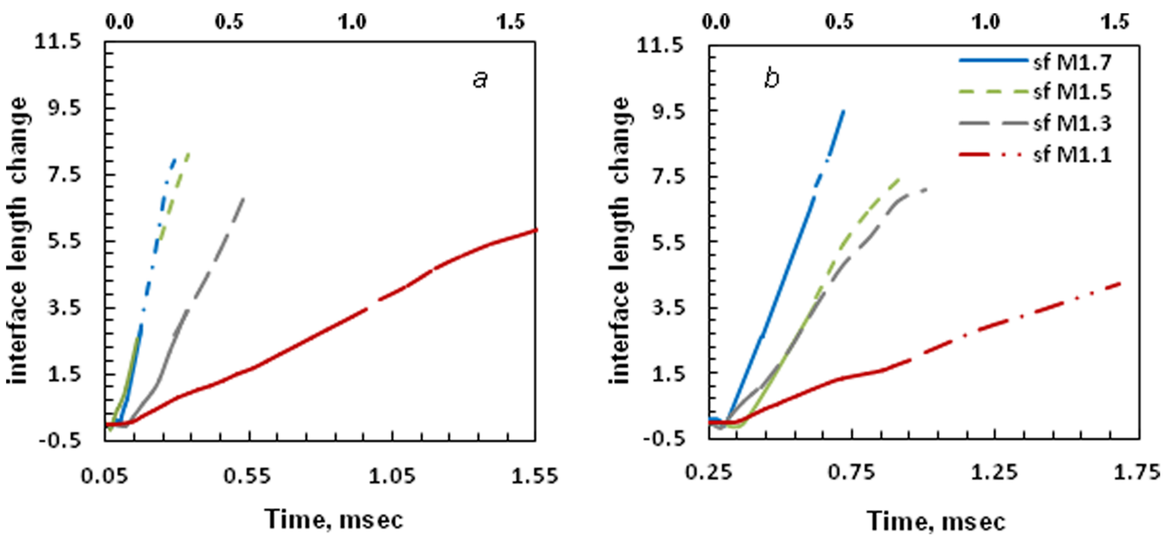

Fig. 9 Interface length change in fast/slow (*a*) and slow/fast (*b*) refractions with various shock strengths ($a_o/\lambda = 0.5$). In slow/fast refraction cases, the interface increase was preceded by a short decrease. The decrease was caused by the interface inversion that started the interface deformation in these cases. Values are normalized by the initial interface length (half-wavelength is 1.38 cm).

Downloaded From: http://fluidsengineering.asmedigitalcollection.asme.org/ on 02/25/2014 Terms of Use: http://asme.org/terms

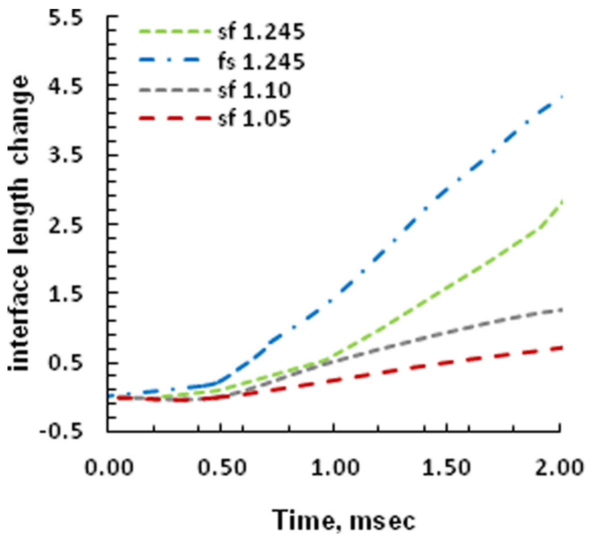

Fig. 10 Sinusoidal interface length increase ($a_o/\lambda = 0.25$) following expansion wave refraction. Values are normalized by the initial interface length (half-wavelength is 1.38 cm).

always accompany it. Moreover, it is possible for part of the interface behind the shock to experience interaction with the reflected waves before the incident shock passes the interface (e.g., in cases with large a_o/λ ratios). Finally, it is the total deposited circulation that may be viewed as a cause of the interface deformation (e.g., following the Biot–Savart law). Considering all of that, values of the deposited circulation were measured after the transmitted shock/expansion wave propagated approximately one perturbation wave length past the interface. For comparison, the circulation, predicted by using the methods of linear stability theory (Eq. (1)) [27], is also shown in Table 2.

$$\Gamma_o = 4a_o \Delta v A \tag{1}$$

where $a_o = (a_{\text{bubble}} + a_{\text{spike}})/2$ is the initial perturbation amplitude, $\Delta v =$ is the interface velocity jump produced by the refraction, and $A =$ the post-shock Atwood number.

The difference between theoretically predicted and numerically measured circulations may be attributed primarily to the effects of secondary vorticity deposition and, to a smaller degree, to the approximations made in the analytical solutions, such as assuming equal specific heat ratios on both sides of the interface and a fixed (preshock) Atwood number.

Now, using the obtained numerical data, we developed a scaling law that relates the interface length increase rate with the key problem parameters.

4 Scaling Law Development

The interface increase following shock or expansion wave refraction has five independent parameters: (1) circulation generated in the refraction (Γ), (2) densities across the interface (ρ_1, ρ_2), (3) perturbation amplitude (a), (4) wave length (λ), and (5) time (t). It is well-known that for infinitely thin interfaces and negligible viscous effects, the exact similarity laws may be used. Simple dimensional analysis based on the Buckingham π theorem yields three dimensionally relevant parameters: one kinematic parameter (dimensionless time $t\Gamma_o/a_o^2$), one dynamic parameter (density ratio ρ_1/ρ_2, which leads to the dimensionless Atwood number), and one geometric parameter (perturbation amplitude-to-wave-length ratio a_o/λ). Therefore, all problem celerities, such as the interface length increase rate (V) expressed in the dimensionless form ($V\lambda/\Gamma_o$), should depend only on these three dimensionless parameters

$$\frac{V\lambda}{\Gamma_o} = f\left[\frac{t\Gamma_o}{a_o^2}, \frac{\rho_1}{\rho_2}, \frac{a_o}{\lambda}\right] \tag{2}$$

Due to the flame-related motivation of this problem, the density ratio may be considered fixed. To gain a further understanding, however, we have to rely on the results of the numerical analysis. As seen in Figs. 8 and 9, the interface length changed almost linearly for an extended period of time until the viscous effects slowed the vortex-like rotational motion or until the translation component of this motion broke the interface into separate segments (Fig. 7).

To our benefit, the nearly constant growth rate of the interface length implies that scaling may be applied at all times

$$\frac{V\lambda}{\Gamma_o} = f\left(\frac{a_o}{\lambda}\right) \tag{3}$$

Table 2 Numerical results summary

Refraction type	Pressure ratio	a_o/λ	V, m/s	Δv, m/s analytical	Γ_o, m^2/s numerical[a]	Γ_o, m^2/s analytical[b]
Shock, fast/slow	3.205	0.250	570	491.0	4.800	3.50
	2.4583	0.250	445	364.7	3.900	2.60
	1.805	0.250	250	231.9	2.800	1.65
	1.245	0.250	66	84.2	1.190	0.60
	2.458	0.500	740	364.7	6.750	5.20
	2.458	0.375	520	364.7	4.230	3.90
	2.458	0.125	195	364.7	1.560	0.60
Shock, slow/fast	3.205	0.250	300	456.2	4.175	3.24
	2.4583	0.250	200	345.7	3.500	2.46
	1.805	0.250	155	223.9	2.700	1.59
	1.245	0.250	44	82.4	1.150	0.59
	2.458	0.125	130	345.7	1.650	1.23
	2.458	0.375	235	345.7	4.850	3.69
	2.458	0.500	245	345.7	6.000	4.92
Expansion, fast/slow	1.245	0.250	75.3		3.040	
	1.1	0.250	22.1		1.340	
	1.05	0.250	12.1		0.740	
Expansion, slow/fast	1.245	0.250	111		3.500	

[a]Circulation was measured after a transmitted shock wave moved a perturbation wave length past the interface.
[b]Computed using analytically estimated velocity jump values.

Downloaded From: http://fluidsengineering.asmedigitalcollection.asme.org/ on 02/25/2014 Terms of Use: http://asme.org/terms

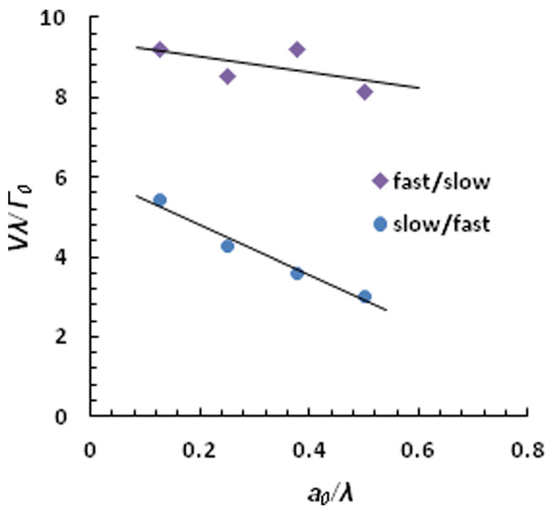

Fig. 11 Dependence of the dimensionless growth velocity on the amplitude-to-wave length ratio in Mach 1.5 shock refractions

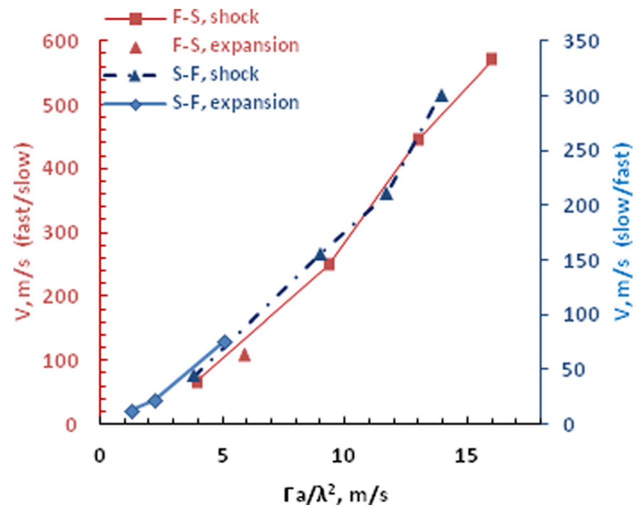

Fig. 12 Rate of interface length change as a function of generated circulation

The above correlation was plotted in Fig. 11 using the computational results with various initial perturbation amplitudes (a_0/λ). However, It should be noted that in the limits of $a_o \rightarrow 0$ the velocity term would also approach zero: $V/\Gamma_o \rightarrow 0$ ($\lambda=$ const). Thus the observed trend should not be valid for the small values of a_o. More importantly, from the results in Fig. 11, it appears that, at least within some range, the function f in Eq. (3) may be approximated as a linear function of the a_o/λ ratio

$$\frac{V\lambda}{\Gamma_o} \approx C_1\left(\frac{a_o}{\lambda}\right) + C_2 \tag{4a}$$

and

$$V \approx \Gamma_o\left[c_1\left(\frac{a_o}{\lambda}\right) + \frac{c_2}{\lambda}\right] \tag{4b}$$

where c_1 and c_2 are some nondimensional constants.

Equation (4a) implies a linear interdependence of V and Γ_o which may be verified by plotting $V = g(\Gamma_o)|_{a\_o,\ \lambda=\text{const}}$. The correlation is plotted in Fig. 12. As expected, the interface length increase rate scales almost linearly with the refraction-produced circulation (Fig. 12). The substitution of Eq. (1) into Eq. (4b) would produce the dependence of the interface increase velocity on the basic problem parameters

$$\begin{aligned} V &\approx \Gamma_o\left[\frac{c_1}{\lambda}\left(\frac{a_o}{\lambda}\right) + \frac{c_2}{\lambda}\right] = 4a_o\Delta vA\left[\frac{c_1}{\lambda}\left(\frac{a_o}{\lambda}\right) + \frac{c_2}{\lambda}\right] \\ &= \Delta vA\left[c_1'\frac{a_o^2}{\lambda^2} + c_2'\frac{a_o}{\lambda}\right] \end{aligned} \tag{5}$$

To interpret the physical meaning of the obtained results, we may recollect that the vorticity generated in either shock or expansion wave refraction produces a vortex-like velocity field (Fig. 7) that stretches the interface in its rotational and translation motion. It can be seen that the interface length increase is proportional to the vortex field rotational velocity. Considering that both the translational and the rotational velocities of the various vortex types (e.g., Lamb–Oseen vortex) linearly depend on circulation [15,28,29], it should have been anticipated that the interface length increase would linearly depend on the generated circulation.

The obtained scaling may also be applicable to the flame theory. Similarly to the normalized interface length change used in the above analysis, the flame stretch rate is equal to the flame length increase rate divided by its length [30].

5 Summary and Conclusions

A dimensional analysis was used to develop a scaling law for the rate of interface length increase following a shock or expansion wave refraction. First, a series of numerical tests was performed with different shock and expansion wave strengths, perturbation amplitudes, and both fast/slow and slow/fast refraction types. A single-mode sinusoidal density interface was employed in this study. To achieve a well-posed problem with a well-defined interface length, the interface was formed by nonreacting gases of different temperatures. The resulting action of the heat diffusion prevented the development of small-scale perturbations at the interface. Considering the main motivation of the problem (shock–flame interaction), the density ratio was assumed to be constant, and its effects were excluded from the analysis. From the remaining problem parameters using the Buckingham π theorem, a function of interest was constructed $V\lambda/\Gamma_o = f\left(t\Gamma_o/a_o^2, a_o/\lambda\right)$ with three dimensionless groups.

Analysis of the numerical results showed that the rate of interface length change remained nearly constant for a significantly longer period of time than the perturbation amplitude growth rate. Velocity of the interface growth is equal to the rate of interface length change. Therefore, this finding allowed us to assume that the velocity of interface length increase is not a function of time, which led to the function form $V\lambda/\Gamma_o = f(a_o/\lambda)$. Based on the numerical results with the variable amplitude-to-wave length rations (a_o/λ), this function could be approximated as a linear function: $V\lambda/\Gamma_o \approx c_1(a_o/\lambda) + c_2$ or $V \approx \Gamma_o[c_1/\lambda(a_o/\lambda) + c_2/\lambda]$. This equation, when combined with the previously derived expression for shock-deposited circulation, may be used to provide the interface increase velocity as a function of the problem's basic parameters: $V = \Delta vA\left[c_1' a_o^2/\lambda^2 + c_2' a_o/\lambda\right]$. The formula was derived from a simple scaling analysis and can be applied to both refraction types (fast/slow and slow/fast) and to both shock and expansion waves.

It has been suggested that the obtained linear correlations of deposited circulation with the rate of interface increase is related to the vortex-like velocity field formed after the refraction. The rotational and translational motion of this flow field is responsible for the interface increase. The linear dependence on circulation emerges from the similar dependence of the rotational and translational velocities of the vortex structures (e.g., vortex ring, Lamb–Oseen vortex) on the circulation.

Downloaded From: http://fluidsengineering.asmedigitalcollection.asme.org/ on 02/25/2014 Terms of Use: http://asme.org/terms

Acknowledgment

Support for this work by Rolls-Royce North American Technologies, Inc. (LibertyWorks) and a doctoral fellowship from the Purdue Research Foundation to the first author is gratefully acknowledged.

References

[1] Rupert, V., 1991, "Shock-Interface Interaction: Current Research on the Richtmyer–Meshkov Problem," Proceedings of the 18th International Symposium on Shock Waves, Sendai, Japan.
[2] Brouillette, M., 2002, "The Richtmyer–Meshkov Instability," Ann. Rev. Fluid Mech., **34**, pp. 445–468.
[3] Zabusky, N., 1999, "Vortex Paradigm for Accelerated Inhomogeneous Flows: Visiometrics for the Rayleigh-Taylor and Richtmyer-Meshkov Environments," Ann. Rev. Fluid Mech., **31**, pp. 495–536.
[4] Matsuoka, C., Nashihara, K., and Fukuda, Y., 2003, "Nonlinear Evolution of an Interface in the Richmyer–Meshkov Instability," Phys. Rev. E., **67**, p. 036301.
[5] Richtmyer, R. D., 1960, "Taylor Instability in Shock Acceleration of Compressible Fluids," Commun. Pure Appl. Math., **13**, pp. 297–319.
[6] Markstein, G. H., 1964, *Nonsteady Flame Propagation*, MacMillan, New York.
[7] Hasegawa, T., Morooka, T., and Nishiki, S., 2000, "Mechanism of Interaction Between a Vortex Pair and a Premixed Flame," Combust. Sci. Technol., **150** (1–6), pp. 115–142.
[8] Scarinci, T., Lee, J. H., Thomas, G. O., Bambrey, R., and Edwards, D. H., 1991, "Amplification of a Pressure Wave by Its Passage Through a Flame Front," Proceedings of the 13th International Colloquium on the Dynamics of Explosions and Reactive Systems, Nagoya, Japan, pp. 3–24.
[9] Khokhlov, A., Oran, E. S., Chtchelkanova, A. Y., and Wheeler, J. C., 1999, "Interaction of a Shock With a Sinusoidally Perturbed Flame," Combust. Flame, **117**(1–2), pp. 99–116.
[10] Ming-Shin, W., and Driscoll, J. F., 1992, "Numerical Simulation of a Vortex Convected Through a Laminar Premixed Flame," Combust. Flame, **91**(3–4), pp. 310–322.
[11] Li, C., and Book, D. L., 1991, "Rayleigh–Taylor Instability Generated by Rarefaction Waves: Comparison With Richtmyer–Meshkov Instability," Proceedings of the 18th International Symposium, Sendai, Japan, July 21–26, pp. 313–318.
[12] Li, D., Sankaran, V., Fakhari, K., and Merkle, C., 2001, "Convergence Assessment of General Fluid Equations on Unstructured Hybrid Grids," Proceedings of the 15th AIAA Computational Fluid Dynamics Conference, Anaheim, CA, AIAA, Paper No. 2001-2557.
[13] Sankaran, V., and Merkle, C. L., 2003, "Artificial Dissipation Control for Unsteady Computations," Proceedings of the 16th AIAA Computational Fluid Dynamics Conference, Orlando, FL.
[14] Li, D., Xia, G., and Merkle, C. L., 2003, "Analysis of Real Fluid Flows in Converging Diverging Nozzles," Proceedings of the 33rd AIAA Fluid Dynamics Conference, Orlando, FL, AIAA, Paper No. 2003-4132.
[15] Kilchyk, V., Nalim, R., and Merkle, C., 2010, "Baroclinic Vorticity Production by Shocks and Expansion Waves," J. Shock Waves, **20**(5), pp. 367–380.
[16] Barth, T. J., and Jespersen, D. C., 1989, "The Design of Application of Upwind Schemes on Unstructured Grids," AIAA, Paper No. AIAA-89-0366.
[17] Gülder, O., and Smallwood, G. J., 1995, "Inner Cutoff Scale of Flame Surface Wrinkling in Turbulent Premixed Flames," Combust. Flame, **103**, pp. 107–114.
[18] Lim, H., Yu, Y., Glimm, J., Li, X. L., and Sharp, D. H., 2008, "Chaos, Transport and Mesh Convergence for Fluid Mixing," Acta Math. Appl. Sin., **24**, pp. 355–368.
[19] Dong, G., Fan, B., and Ye, J., 2008, "Numerical Investigation of Ethylene Flame Bubble Instability Induced by Shock Waves," Shock Waves, **17**(6), pp. 409–419.
[20] Kilchyk, V., Nalima, R., and Merkle, C., 2011, "Laminar Premixed Flame Fuel Consumption Rate Modulation by Shocks and Expansion Waves," Combust. Flame, **158**(6), pp. 1140–1148.
[21] Akbari, P., and Nalim, M. R., 2009, "Review of Recent Developments in Wave Rotor Combustion Technology," AIAA J. Propul. Power, **25**(4), pp. 833–844.
[22] Samtaney, R., and Zabusky, N., 1993, "On Shock Polar Analysis and Analytical Expressions for Vorticity Deposition in Shock-Accelerated Density-Stratified Interfaces," Phys. Fluids A, **5**(6), pp. 1285–1287.
[23] Samtaney, R., Ray, J., and Zabusky, N., 1998, "Baroclinic Circulation Generation on Shock Accelerated Slow/Fast Gas Interfaces," Phys. Fluids, **10**(5), pp. 1271–1285.
[24] Zucrow, M. J., and Hoffman, J. D., 1976, *Gas Dynamics*, Vol. 1, John Wiley & Sons, New York.
[25] Sadot, O., Erez, L., Alon, U., Oron, D., Levin, L. A., Erez, G., Ben-Dor, G., and Shvarts, D., 1998, "Study of Nonlinear Evolution of Single-Mode and Two-Bubble Interaction Under Richtmyer–Meshkov Instability," Phys. Rev. Lett., **80**, pp. 1654–1657.
[26] Peng, G.-Z., Zabusky, N. J., and Zhang, S., 2003, "Vortex-Accelerated Secondary Baroclinic Vorticity Deposition and Late Intermediate Time Dynamics of a Two-Dimensional Richtmyer–Meshkov Interface," Phys. Fluids, **15**(12), pp. 3730–3744.
[27] Jacobs, J. W., and Sheeley, J. M., 1996, "Experimental Study of Incompressible Richtmyer–Meshkov Instability," Phys. Fluids, **8**, pp. 405–416.
[28] Saffman, P. G., 1992, *Vortex Dynamics, Cambridge Monographs on Mechanics and Applied Mathematics*, Cambridge University Press, Cambridge, UK.
[29] Howe, M. S., 2007, *Hydrodynamics and Sound*, Cambridge University Press, Cambridge, UK.
[30] Poinsot, T., and Veynante, D., 2005, *Theoretical and Numerical Combustion*, R.T. Edwards, Inc., Philadelphia, PA.

Downloaded From: http://fluidsengineering.asmedigitalcollection.asme.org/ on 02/25/2014 Terms of Use: http://asme.org/terms